

## Preparation of Chemically Modified Porous Carbon Networks Derived from Citrus Sinensis Flavedos as Electrode Material for Supercapacitor

Malathi Devendran<sup>1</sup>, Senthil Kumar Kandasamy<sup>1,\*</sup>, Shanmugam Palanisamy<sup>2</sup>, Sangavi Selvaraj<sup>1</sup>, Ragavi Vetrivel<sup>1</sup>, Roobak Selvarajan<sup>1</sup>, Murugesan Govindasamy<sup>1</sup>, Kannan Kandasamy<sup>2</sup>

<sup>1</sup> Department of Electronics and Communication Engineering, Kongu Engineering College, Erode-638060, India

<sup>2</sup> Department of Chemical Engineering, Kongu Engineering College, Erode-638060, India

\*E-mail: [senthilkumar6k@gmail.com](mailto:senthilkumar6k@gmail.com)

Received: 22 November 2019/ Accepted: 13 February 2020 / Published: 10 April 2020

---

This work has mainly focused on the development of a type of porous nitrogen doped carbon networks derived from green biomass waste (citrus sinensis flavedos) by carbonization and activation. Different chemical activations using sulphuric acid, hydrochloric acid and phosphoric acid are employed to obtain improved specific capacitance. From the XRD results, broad peak was observed at 24°. The performance of citrus sinensis flavedos derived carbon materials for supercapacitor applications is evaluated using aqueous electrolyte (0.5 M H<sub>2</sub>SO<sub>4</sub>) at various current densities and scan rate of 30 mV.s<sup>-1</sup>. The superior performance of the derived nanoporous carbon is attributed to high surface area with fast ionic and electronic diffusion of the electrolyte in and out of the pores. From CV analysis, the electrodes OPC, OPCH, OPCP and OPCS in 0.5 M H<sub>2</sub>SO<sub>4</sub> aqueous electrolyte exhibit the specific capacitance of 39, 28, 92 and 88 F.g<sup>-1</sup> respectively, with improved capacity retention ratio. From GCD measurement, the specific capacitances are calculated as 52, 19, 169 and 35 F.g<sup>-1</sup> for OPC, OPCH, OPCP and OPCS respectively at 0.25 mA.g<sup>-1</sup>. When compared to chemically activated samples, pure citrus sinensis flavedos exhibited small equivalent series resistance.

---

**Keywords:** Citrus Sinensis Flavedo, Chemical Activation, Supercapacitor, Specific Capacitance

### 1. INTRODUCTION

In this modernized world, the population is surging in a tremendous manner. Hence the energy consumed and the depletion of energy is increasing progressively. Renewable energy sources have to trap for the growing energy demand and substitute alternative for energy depletion. There are two way in utilizing the renewable energy, such as; 1) Direct use in energy integrated system and 2) indirect use

in harvesting energy through stored devices. Energy storage devices are required to store the energy in either chemical form or in an electric field. The most common energy storage devices address is batteries and capacitors. Though these devices are vital in storage of energy, there are some of the cons concerned with these devices such as energy density of capacitors and the power density of batteries are very much low. Thus, supercapacitors involved into an existence that is used to bridge the gap between capacitors and batteries.

Supercapacitors, are the energy storage devices, that have been drawing more attention because of its advantages [1]. The supercapacitors have high energy density when compared with capacitors and high-power density when compared with batteries. Supercapacitors, known as electrochemical capacitors, are capable of providing fast and reversible redox reactions in high charging and discharging rates, cycling stability and current capacity. Due to these pros characterized by the supercapacitor, they are used in multidisciplinary areas such as military devices, hybrid electric vehicles such as cars and cranes, burst-mode electronic devices, trains and elevators.

Supercapacitors are classified into two type's namely electrochemical double layer capacitor (EDLC) and pseudocapacitors. The most commonly identified supercapacitor is EDLCs. This is because EDLCs use varieties of carbon materials as an electrode. As activated carbon possesses high surface area, the energy stored in EDLC is higher [2]. Conducting polymer composite [3-4] with graphene oxide can be one of the effective methods to improving the specific capacitance. The activated carbon is used as an electrode for EDLCs due to its large surface area, affordable cost and availability of standard synthesis methods. This carbon is usually prepared from various biomass sources such as cycas leaves [5], corn straw [6-7], neem leaves, potato [8-10], banana peels [11-14], flavedos of orange [15-24], walnut shells, rice husk [25], rotten carrot, and pineapple leaves. The most commonly used precursors for activating carbon are Nitric acid, Sulphuric acid and Hydrochloric acid. An orange-peel-based supercapacitor demonstrated high performance by reaching a high specific capacitance, high power density and high energy density [26].

In this work, the carbon is synthesised from citrus sinensis flavedos and is the source material for the electrodes used in supercapacitor. The carbon is then activated using activating agents like nitric acid, sulphuric acid and hydrochloric acid. The structure parameters of the samples are analysed using XRD pattern and FTIR. The electrochemical measurements of the carbon as well as the activated carbon are studied using Cyclic Voltammetry (CV), Galvanostatic Charge Discharge measurement (GCD) and Electrochemical Impedance Spectroscopy (EIS).

## 2. EXPERIMENTAL SECTION

### 2.1. Materials used:

Fresh orange fruits (Citrus Sinensis) are purchased from local shop located in Tirupur, Tamilnadu, India. HCl, H<sub>2</sub>SO<sub>4</sub> and H<sub>3</sub>PO<sub>4</sub> are obtained from Sigma Aldrich, India. All the solutions are prepared using deionised water.

## 2.2. Preparation of Orange peels derived activated carbon:

Fresh orange peels are extracted from the purchased orange fruits and sliced with appropriate dimensions for simple activation. The peels are dried at 100°C for 12 hours in hot air oven. The pre-carbonized orange peel is grinded and sieved with particle size less than 1 mm in mesh strainer. These samples were carbonized at 600°C in muffle furnace under N<sub>2</sub> gas atmosphere, at a constant flow rate of 1 litre per minute for a period of 3 hrs. This material is kept overnight under CO<sub>2</sub> atmosphere at room temperature. Then the prepared material is named as OPC. The collected carbon was grounded into powder and rinsed with 1 M of HCl, H<sub>2</sub>SO<sub>4</sub> and H<sub>3</sub>PO<sub>4</sub> and respectively named as OPCH, OPCS and OPCP. The powder samples are dried at 60°C for 24 hrs. Finally, the chemically activated carbon is neutralized around pH=7.0 after several washing with deionized water.

## 2.3. Structural and electrochemical characterization of OPC, OPCH, OPCS and OPCP:

The notification of XRD patterns using miniflex and smart-lab Rigaku diffractometer on activated carbon are recorded between 10° and 90° with copper radiation sources. Surface functionalities of the prepared OPC, OPCH, OPCS and OPCP are identified using FTIR (Bruker FTIR A.Model Tensor-27). Electrochemical properties are measured by Cyclic Voltammetry using Orignalys electrochemical work station at room temperature (25°C). The graphite rod has considered as the working electrode. To prepare the working electrode, the samples are mixed with the rubber solution and made slurry. Then the slurry is coated on graphite rod. A Pt wire and Ag/AgCl electrode have used as counter and reference electrodes, respectively. CV is recorded in 0.5 M H<sub>2</sub>SO<sub>4</sub> aqueous solution at a scan rate of 30 mV.s<sup>-1</sup>. For analysing the performance of supercapacitor, the electrode is prepared as reported in the previous study [5]. An equivalent series resistance and charge transfer resistance of the OPC, OPCH, OPCS and OPCP samples are measured by using electrochemical impedance spectroscopy.

## 3. RESULTS AND DISCUSSION

The crystalline nature of OPC, OPCH, OPCS and OPCP samples are characterized by XRD method. The XRD pattern of OPC, OPCH, OPCS and OPCP samples are shown in Figure 1. The diffraction pattern of the samples reveals a broad peak at 24° and a weak band at 41° corresponds to the (002) and (100) respectively. Small changes are observed between the samples. The broad peak appeared in XRD identifies the amorphous carbon structure. When compared with OPC, the peak intensity of remaining samples have shown weak, indicated that the graphitization degree decreases. FTIR spectroscopy techniques enable to identify functional groups, organic compound, structure determination and study of chemical groups. Figure 2 shows the intensity measured in transmittance at FTIR of OPC, OPCH, OPCS and OPCP. FTIR analysis is used to further understand the effects of chemical activation on OPC. The samples are individually mixed with KBr powder for tablet preparation and then placed for analyzing in FTIR spectroscopy. The range of the spectrum is observed from 400 to 4000 cm<sup>-1</sup>. The spectra shows the important characteristic bands related to cellulose

besides of lignin. In the high energy region, the broad and intense band around  $3560\text{ cm}^{-1}$  are observed due to OH stretching vibrations of lignin and carbohydrates [26]. The bending vibrations around  $1474\text{ cm}^{-1}$  formed the structure of this material. The band at  $1742\text{ cm}^{-1}$  and  $1734\text{ cm}^{-1}$  are ascribed to C=O stretching band of carboxy groups [26]. The peaks at  $3741\text{ cm}^{-1}$  and  $3587\text{ cm}^{-1}$ , are higher than the peak at  $3561\text{ cm}^{-1}$  indicated an increased hydroxyl groups on the surface area after chemical activation. The band at  $1510\text{ cm}^{-1}$  ascribed to aromatic skeletal stretching band. The band at  $1417\text{ cm}^{-1}$  corresponds to weak intensity of hydroxyl group band.

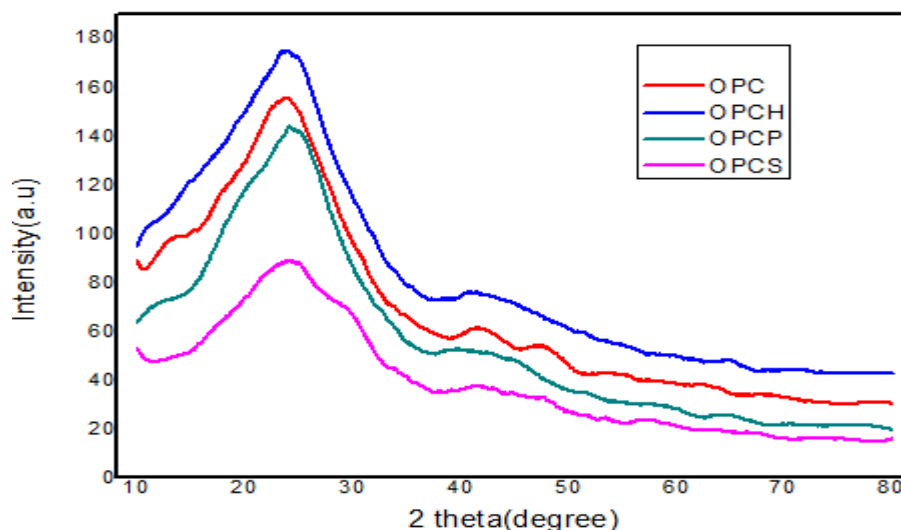


**Figure 1.** X-Ray Diffraction patterns of OPC, OPCH, OPCR and OPCS

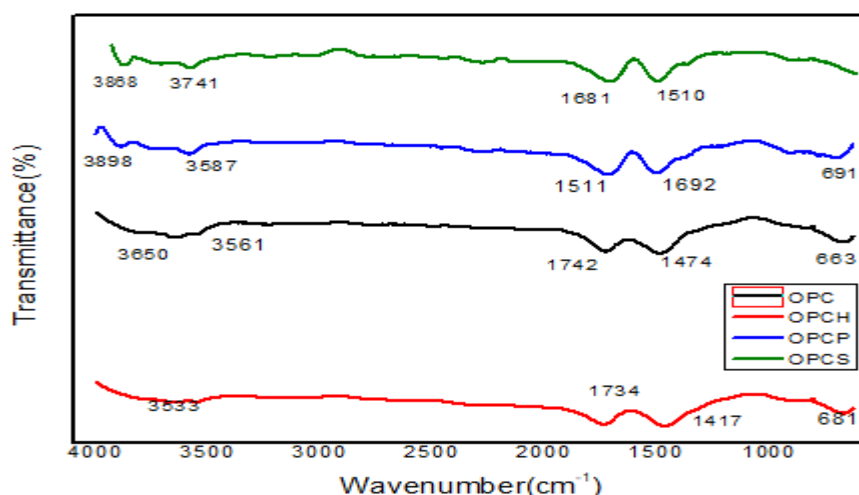


**Figure 2.** Fourier Transform Infrared spectra of OPC, OPCH, OPCS and OPCR

The electrochemical performance of OPC, OPCH, OPCS and OPCR samples have analysed using CV between 0 mV to +2000 mV (vs. Ag/AgCl), GCD between -600 mV to +1400 mV (vs. Ag/AgCl) and EIS in a three-electrode configuration. The area under the CV curve of OPCH electrode show higher than other electrodes, which indicate the improvement in the electrochemical energy

storage and the rectangular curve indicates the EDLC and small amount of pseudocapacitance by the OPCH electrode. To optimize the activating agents, CV can be measured for OPCP, OPCS and OPCH and shown in Figure 3 (a). Among the three chemically activated orange peel-based electrodes, the CV profile of OPCP electrode has shown excellent electrochemical performance compared to OPCH and OPCS electrodes.

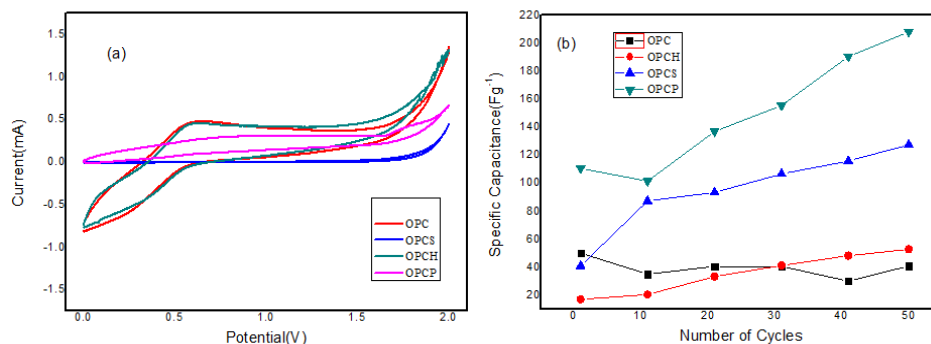


**Figure 3.** (a) Cycle Voltammetric curves of as prepared samples at a scan rate of  $30 \text{ mV.s}^{-1}$ , (b) Cycling performance of OPC, OPCH, OPCP and OPCS

Because of the pseudocapacitance, EDLC with faradaic hump is observed for OPC and OPCH electrodes. But, OPCS and OPCP show only the EDLC curve, minimization of functional groups due to the sulphuric acid and phosphoric acid chemical activation on orange peel powder. The specific capacitances are measured as 39, 28, 92 and  $88 \text{ F.g}^{-1}$  respectively, corresponding to OPC, OPCH, OPCP and OPCS. The cycling stability have tested on the prepared samples for 50 cycles and shown in Figure 3 (b). All the electrodes have shown improved specific capacitance up to 50 cycles. Among the different electrodes, OPCP have noticed highest specific capacitance ratio and excellent stability at 50<sup>th</sup> cycle.

To analyze the capacitive performance of citrus sinensis flavedos and its chemical activation, its electrochemical properties are analysed at different current densities using galvanostatic charge and discharge measurement. The GCD curves of citrus sinensis flavedos are shown in Figure 4. The curves are approximately a triangular shape with small amount of IR drop can be observed for OPC, OPCP and OPCH. The curve displays an almost isosceles triangular shape with zero amount of IR drop has been observed at  $0.25 \text{ mA.g}^{-1}$ . The specific capacitances are calculated as 72, 65, 59 and  $50 \text{ F.g}^{-1}$  for OPC, OPCH, OPCP and OPCS respectively at  $0.025 \text{ mA.g}^{-1}$ . Similarly, the specific capacitances are calculated as 67, 47, 64 and  $51 \text{ F.g}^{-1}$  for OPC, OPCH, OPCP and OPCS respectively at  $0.05 \text{ mA.g}^{-1}$ ; and 63, 33, 77 and  $47 \text{ F.g}^{-1}$  for OPC, OPCH, OPCP and OPCS respectively at  $0.1 \text{ mA.g}^{-1}$ ; and 52, 19, 169 and  $35 \text{ F.g}^{-1}$  for OPC, OPCH, OPCP and OPCS respectively at  $0.25 \text{ mA.g}^{-1}$ . The higher specific capacitance ( $169 \text{ F.g}^{-1}$  at  $0.25 \text{ mA.g}^{-1}$ ) is observed for OPCP electrodes. Compared to normal activation [22], OPCP exhibited highest specific capacitance, because of low equivalent series resistance. From the results, citrus sinensis flavedos can be used as low cost biomass based activated carbon source for electrochemical supercapacitors, especially when it is activated using phosphoric acid.

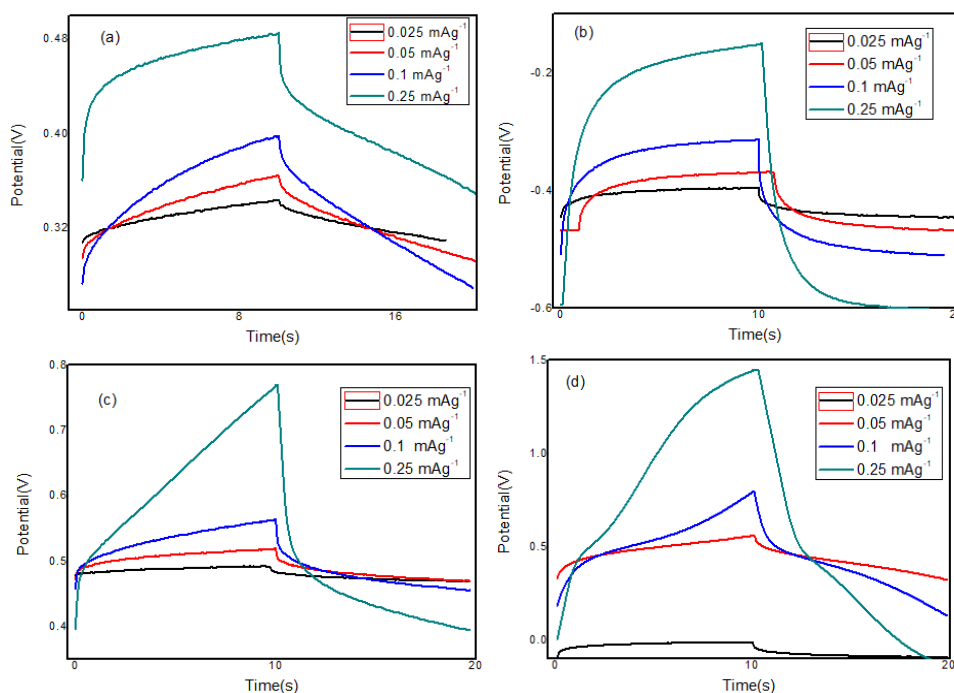


**Figure 4.** Galvanostatic Charge and Discharge spectra of (a) OPC (b) OPCP (c) OPCS and (d) OPCH

To further investigate the transport kinetics and ion diffusion, electrochemical impedance spectroscopy has been employed. The nyquist curve is plot within the frequency range of 100 kHz to 0.1 Hz which is shown in Figure 5. The series resistance and charge transfer resistance of the samples is measured from the semicircle and it is tabulated in Table 1. From the  $R_{ct}$  values, the ion transport for the samples can be estimated.

**Table 1.** Series resistance and charge transfer resistance of prepared samples from electrochemical impedance spectroscopy

	OPC	OPCS	OPCH	OPCP
$R_s$ ( $\Omega$ )	1.08	61.15	87.90	39.09
$R_{ct}$ ( $\Omega$ )	2.04	5.52	4.68	3.41

All the prepared samples exhibited the linear curve in the low frequency region except OPC, corresponds to excellent capacitive performance. When compared to chemically activated samples, normal OPC exhibits lower equivalent series resistance (1.08  $\Omega$ ). The result indicates that it has been suggested the high electrode conductivity for OPC [22]. Among the samples, OPCH exhibited very high  $R_s$ , because of the hydrochloric acid activation on orange peel-based carbon may have a smaller number of pores and charge transport. At the same time, phosphoric acid activation improves the porous structure and enhanced the charge transport. Even though, OPCP exhibited high  $R_s$  than OPC sample, due to the chemical activation it exhibited high specific capacitance than OPC. Table 2 gives the various electrochemical parameters of electrodes. From the Table 2, it is observed that the orange

peel derived activated carbon has enough potential to act as electrodes in supercapacitor, because of its specific capacitance and capacity retention ratio.

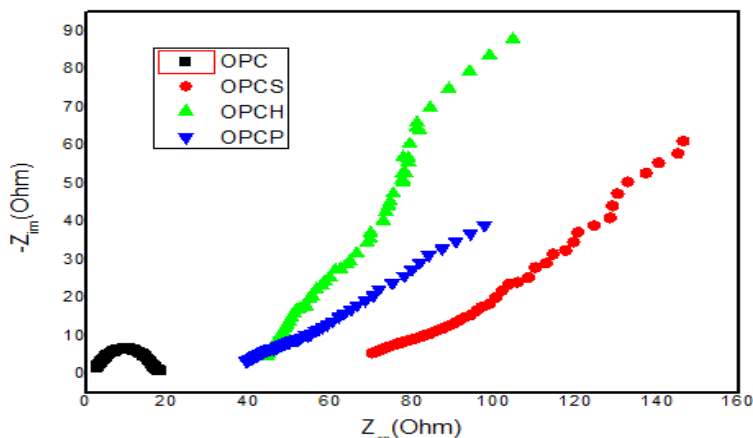


Figure 5. Nyquist plots of OPC, OPCS, OPCH and OPCP

Table 2. Various electrochemical parameters of orange peel derived activated carbon

S. No	Synthesis Process	Specific Capacitance	Electrolyte	Capacity Retention Ratio	Series and Charge Transfer Resistance	Ref. No
1	Integrated carbonization, activation and nitrogen doped process	255 F.g <sup>-1</sup> at 0.5 A.g <sup>-1</sup>	6 M KOH	96 % after 5000 charge/discharge cycles	---,---	14
2	Activation and carbonization	460 F.g <sup>-1</sup> at 1 A.g <sup>-1</sup>	Aqueous	98 % after 10000 charge/discharge cycles	0.25, 0.3 Ω	16
3	Carbonization	656 F.g <sup>-1</sup> at 1 A.g <sup>-1</sup>	---	Above 80 % after 5000 charge /discharge cycles	---,---	18
4	Pyrolysis and chemical activation	217 F.g <sup>-1</sup> at 1 A.g <sup>-1</sup>	3 M KOH	Above 100 % after 5000 charge /discharge cycles	---, 0.36 Ω	21
5	Carbonization	168 F.g <sup>-1</sup> at 0.7 A.g <sup>-1</sup>	6 M KOH	---	1.53, 1.87 Ω	22
6	Chemical Activation and carbonization	169 F.g <sup>-1</sup> at 0.25 mA.g <sup>-1</sup>	0.5 M H <sub>2</sub> SO <sub>4</sub>	Above 100 % after 50 charge /discharge cycles	1.08, 2.04 Ω	This work

#### 4. CONCLUSION

By carbonization and activation, nitrogen doped carbon with a well-developed porous structure can be synthesized from readily available flavedodos of waste citrus sinensis. The orange peel derived

carbon can further activate using sulphuric acid, hydrochloric acid and phosphoric acid in order to obtain improved specific capacitance. The performance of citrus sinensis flavedos derived nanoporous activated carbon materials for supercapacitor applications is evaluated using 0.5 M H<sub>2</sub>SO<sub>4</sub> at various current densities such as 0.25, 0.1, 0.05, 0.025 mA.g<sup>-1</sup> and scan rate of 30 mV.s<sup>-1</sup>. The superior performance of citrus sinensis flavedos derived nanoporous carbon is mainly attributed to high surface area and porous nature of chemically activated biowaste. From the XRD results, it is recognized that the materials are crystalline in nature with a broad peak at 24°. Among all the samples, OPCP exhibited the specific capacitance of 92 F.g<sup>-1</sup> from CV analysis, 169 F.g<sup>-1</sup> specific capacitance from GCD analysis, and the series resistance of 39.09 Ω. For high performance of sustainable and cheap energy storage device, an appropriate activating agent (phosphoric acid) can be identified from the electrochemical measurements.

#### ACKNOWLEDGEMENT

The authors thank the FIST, Department of Science and Technology (SR/FST/COLLEGE-096/2017), India for financial support.

#### References

1. D. Sivalingam, H. Elangovan, M. Subramanian, S.K. Kandasamy and M. Govindasamy, *Adv. Mater. Res.*, 768 (2013) 334.
2. C. Xu, F. Xu, L. Sun, L. Gao, F. Yu, H. Zhang, E. Yan, H. Peng, H. Chu and Y. Zou, *Int. J. Electrochem. Sci.*, 14 (2019) 1782.
3. G. Shi, Y. Dong, G. Wang, X. Jiang, C. Liu, S. Jia, P. Zhang and H. Ma, *Int. J. Electrochem. Sci.*, 13 (2018) 4020.
4. S. K. Kandasamy and K. Kandasamy, *J. Inorg. Organometallic Polymers & Mat.*, 28 (2018) 559.
5. S. K. Kandasamy and K. Kandasamy, *Int. J. Electrochem. Sci.*, 14 (2019) 4718.
6. W. Cao, E. Zhang, J. Wang, Z. Liu, J. Ge, X. Yu, H. Yang and B. Lu, *Electrochem. Acta*, 293 (2019) 364.
7. M. Yadav, M. Kumar and N. Srivastava, *Electrochem. Acta*, 283 (2018) 1551.
8. Y. Yan, Y. Wei, Q. Li, M. Shi, C. Zhao, L. Chen, C. Fan, R. Yang and Y. Xu, *J. Mat. Sci: Mat. Electron.*, 29 (2018) 11325.
9. I. Kaushal, S. Maken and A.K. Sharma, *Korean Chem. Engg. Res.*, 56 (2018) 694.
10. A. Rahmah, A. Zainollah, N.A. Fitriani, D. Sapri, Ramadhan, M. Cahayo and Masruroh, *Indonesian J. Appl. Phys.*, 7 (2017) 46.
11. E. Taer, R. Taslim, Z. Aini, S.D. Hartati and W.S. Mustika, *AIP Conf. Proc.*, 4 (2017) 1.
12. O. Fasakina, J.K. Dangbegnon, D.Y. Momodub, M.J. Madito, K.O. Oyedotun, M.A. Eleruja and N. Manyala, *Electrochim. Acta*, 262 (2018) 187.
13. K.H. Teoh, C.S. Lim and C.W. Liew, Rameshsingh, *Ionics*, 21 (2018) 2061.
14. H. Gou, J. He, G. Zhao, L. Zhang, C. Yang and H. Rao, *Ionics*, 1 (2019) 1-10.
15. X. Chan, K.M. Wu, B. Gao, Q. Xiao, J. Kong, Q. Xiong, X. Peng, X. Zhang and J. Fu, *Waste Biomass Valor.*, 7 (2016) 551.
16. K. Subramani, N. Sudhan, M. Karnan and M. Sathish, *Energy Tech. Environ. Sci.*, 2 (2017) 11384.
17. K. Subramani and M. Sathish, *Sci. Rep.*, 9 (2019) 1.
18. K. Sun, H. Wang, H. Peng, Y. Wu, G. Ma and Z. Lei, *Int. J. Electrochem. Sci.*, 10 (2015) 2000.
19. D. Liu, W. Zhang and W. Huang, *Chin. Chem. Lett.*, 30 (2019) 1315.

20. M. Deraman, N.S. Mohd Nor, E.T.B. Yatim, Awitdrus, Rakhmawati Farma, N.H. Basri, M.R.M. Jasni, Rusli Dalik, S. Soltaninejad, M. Suleman, G. Hedge and A.A. Astimar, *MSF*, 846 (2018) 497.
21. C.K. Ranveera, P.K. Kahol, M. Ghimire, S.R. Mishra and R. K.Gupta, *J. Carbon Res.*, 3, (2017) 1.
22. S. Ahmed, M. Rafat and A. Ahmed, *Adv. Nat. Sci: Nanosci. Nanotech.*, 9 (2018) 1.
23. B. Zapata, J. Balmaseda and E. Fregoso-Israel, *J. Therm. Anal. Calorim.*, 98 (2009) 309.
24. M. Puccini, D. Licursi, E. Stefanalli, S. Vitolo, A. M .R. Galletti and H.J. Heeras, *Chem. Eng. Trans.*, 50 (2016) 223.
25. R.S.Orozco, P. B. Hernandez, N. F. Ramirez, G. R. Morales, J. S. Luna and A. J. C. Montoya, *Appl. Biochem. Biotechnol.*, 176 (2015) 758.
26. P. J Li, J. L. Xia, Y. Shan, Z. Y. Nie and F. R. Wang, *Appl. Biochem. Biotech.*, 176 (2015) 1

© 2020 The Authors. Published by ESG ([www.electrochemsci.org](http://www.electrochemsci.org)). This article is an open access article distributed under the terms and conditions of the Creative Commons Attribution license (<http://creativecommons.org/licenses/by/4.0/>).